

Tropos, Nevertheless Conformationally Stable Biphenyl Derivatives

Gebhard Haberhauer,^{*[a]} Christina Tepper,^[a] Christoph Wölper,^[a] and Dieter Bläser^[a]

Keywords: Chirality / Atropisomerism / CD spectroscopy / Conformation analysis / Molecular modeling / Biaryls / Macrocycles

Biphenyl derivatives with small substituents in the *ortho* and *ortho'* positions are called *tropos*. Due to the low rotation barrier around the C–C bond connecting the two phenyl units, the isolation of only one conformer is not possible; thus they are conformationally unstable. Using DFT calculations, we were able to show that using a suitable peptidic bridging unit, biphenyl systems can become conformationally stable. This stabilization should be independent of the type of sub-

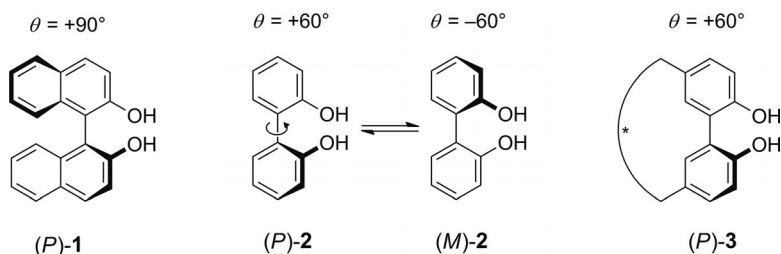
stituent in the *ortho* and *ortho'* positions. Some of the proposed biphenyl derivatives were successfully synthesized and studied in solution and solid state. The recorded VT-NMR, 2D-NMR and CD spectra show that all biphenyl derivatives exhibit the *P* conformation. The preference for the *P* conformation is confirmed by the structure of a biphenyl derivative in solid state.

Introduction

Biphenyls and their congeners (biaryls) are elemental building blocks in asymmetric synthesis, asymmetric catalysis and chiral supramolecular chemistry.^[1–3] The intrinsic chirality in these systems results from the fact that coplanarity of the two phenyl or aryl rings leads to repulsive interactions between the substituents in the *ortho* and *ortho'* positions, and is thus avoided. Depending on the dynamic behavior, the biphenyls are divided into *tropos* and *atropos* systems.^[4] If the two enantiomers can be isolated at 300 K, they are called *atropos*. This isomerism caused by blocking the internal rotation around a single bond is named atropisomerism. If the interconversion via planar conformation is too fast to isolate chiral axial enantiomers, the system is called *tropos*. Oki has discussed the borderline between *tropos* and *atropos* in more detail.^[5] The minimum require-

ment for *atropos* biphenyls is a rotation barrier of more than ca. 93 kJ mol⁻¹. If such a high or even higher rotation barrier is present, the isolation of enantiomers at 300 K is possible.

A very important example of *atropos* biaryls is the compound BINOL (**1**; Scheme 1) and its derivatives which found wide application in enantioselective synthesis and catalysis.^[1,2,6] Furthermore, due to their clearly defined chiral structure, they are widely used as chiral building blocks in supramolecular chemistry.^[3] The enormous advantage in the use of *atropos* biaryls is the fact that they do not racemize. The disadvantage of *atropos* biaryl systems is their rigid structure; the dihedral angle θ around the chiral axis is usually around 90°. This is due to the fact that *atropos* biaryl systems normally carry four substituents in the *ortho* positions to the carbon atoms connecting the two aryl rings. If the size or the number of *ortho* substituents is reduced,



Scheme 1. *Atropos* (**1**) and *tropos* (**2** and **3**) biaryl systems.

[a] Institut für Organische Chemie, Fakultät für Chemie, Universität Duisburg-Essen, Universitätsstraße 7, 45117 Essen, Germany
E-mail: gebhard.haberhauer@uni-due.de
Homepage: <http://www.uni-due.de/akhaberhauer/>

Supporting information for this article is available on the WWW under <http://dx.doi.org/10.1002/ejoc.201300087>.

the whole system becomes more flexible and dihedral angles θ smaller than 70° are observed (see for example **2** in Scheme 1).^[7] However, this modification also leads to a decrease of the rotation barrier, and thus the system becomes *tropos*, and racemization is observed. So, if a *tropos* ligand

should be used in chiral catalysis, it must be combined with a second element showing permanent chirality.^[8]

One way out of this dilemma is the introduction of a chiral bridge in the *meta* positions to the carbon atoms connecting the two aryl rings,^[9] as depicted in compound **3** in Scheme 1. This bridge has to comply with two requirements: on one hand it must be flexible enough to allow the system to adopt a conformation with a dihedral angle of about 60°, and on the other hand it must be rigid enough to adopt only one conformation in solution. In the case of compound **3**, the *P* conformation is depicted.^[10]

There are several attempts reported in the literature to stabilize one isomer of *ortho* disubstituted biphenyls by introduction of an additional chiral unit. To our best knowledge, these attempts were only successful for large substituents or within supramolecular structures,^[11] but failed for smaller ones like hydroxy groups.^[12] Herein we describe a strategy to control the axial chirality in *tropos* biphenyl systems which is independent of the nature of the *ortho* substituents.

Results and Discussion

Concept and Calculations

In order to test which chiral bridge best fulfills the requirements, ab initio calculations for three different chiral bridges (*A–C*) and for five different biphenyl units (**a–e**) were performed (Figure 1).^[13] System **C** is a modification of BINOL in which the carbon atoms in the *meta* positions are used as connection units between chiral bridge and biphenyl unit. The bridges **A** and **B** are peptidic macrocycles^[14] and differ only in the methyl groups at the imidazole rings; the configuration at all stereogenic carbon atoms is the same. Despite the large number of single and amide bonds in the scaffold, imidazole-containing cyclopeptides are rigid and adopt only a single conformation in solution.^[15] Therefore they have been already successfully used for chirality induction in *C*₂- and *C*₃-symmetric systems, as chiral receptors, and in chiral molecular devices.^[16] Hence, we expected that these imidazole-containing peptides would fulfill the above-mentioned requirements. All geometries of the *P* and *M* isomers of **4–6** were com-

pletely optimized using the B3LYP/6-31G* level of theory. In Table 1 the calculated energy differences between the *P* and *M* isomers of **4–6** are listed.

Table 1. Energy difference, ΔE in kJ mol⁻¹, between the *P* and *M* isomers of **4–6** and the dihedral angles $\theta_{\text{CR-C-C-CR}}$ [°] of the lower-energy conformer calculated using B3LYP/6-31G*.

	R	4		5		6	
		ΔE	θ	ΔE	θ	ΔE	θ
a	H	8.1	+40	-10.9	-61	0.1	+41
b	OH	13.5	+51	-15.3	-51	5.0	+50
c	OMe	16.4	+63	-15.2	-61	4.3	+63
d	Me	23.5	+70	-13.3	-67	3.8	+69
e	Br	28.4	+71	-9.6	-70	4.8	+71

A comparison between the three bridges *A–C* reveals that in all systems an energetic discrimination between the diastereomeric isomers *M* and *P* exists. However, for the binaphthyl derivatives **6** (bridge **C**) the calculated differences are small. For example, for **6a** (R = H), almost no preference for one conformation is found ($\Delta E = 0.1$ kJ mol⁻¹). For the bridges **A** and **B**, the energetic discrimination is pronounced for all studied substituents. However, the bridges **A** and **B** show different trends. In the case of bridge **A**, the *P* isomer is the energetically more stable one, and stabilization of the *P* conformation increases with increasing size of the substituent. For example, compound **4a**, with H in the *ortho* and *ortho'* positions, shows the smallest energy difference, ($\Delta E = 8.1$ kJ mol⁻¹) and **4e**, which has bromine substituents in the *ortho* and *ortho'* positions shows the highest energetic discrimination ($\Delta E = 28.4$ kJ mol⁻¹). In contrast, for bridge **B**, the energetic difference between the conformers decreases with increasing size of the substituent, and in all cases, the *M* conformers are the more stable ones. An explanation for this behavior is the interaction between the methyl group at the imidazole ring (bridge **A**) and the biphenyl unit. In the case of the *M* conformers the phenyl ring points toward the methyl group, leading to steric repulsion. With increasing size of the substituents, the dihedral angle between the phenyl rings increases and the phenyl units are pushed even further to the methyl group. Thus, the energetic preference for the *P* conformers rises. Without a methyl group (bridge **B**), the *M* conformers are preferred. As expected, the calculated dihedral angles $\theta_{\text{CR-C-C-CR}}$ of the tethered biphenyl compounds are distinctly smaller than

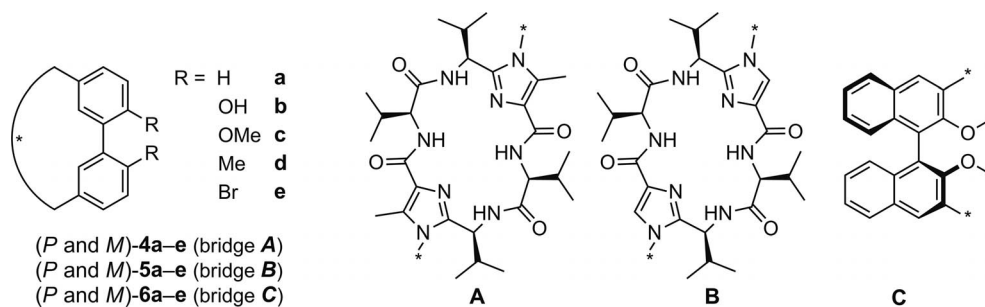


Figure 1. The biphenyl systems **4–6** consist of a biphenyl unit exhibiting a substituent R in the *ortho* and *ortho'* positions and a chiral bridge (*A–C*) in the *meta* positions.

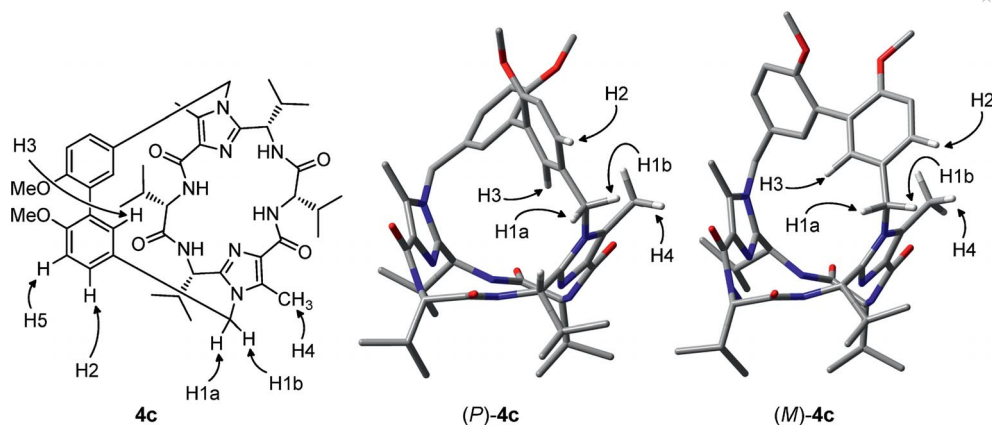


Figure 2. Formula of **4c** and molecular structures of the isomers (*P*)-**4c** and (*M*)-**4c** calculated by using B3LYP/6-31G*. Most of the hydrogen atoms were omitted for clarity.

those found in the corresponding tetra-*ortho*-substituted *atropos* biaryls, which often display angles of 90° or higher.^[17]

The geometry-optimized isomers of **4c** are depicted in Figure 2. In both cases, the peptidic scaffold exhibits a bowl-like and slightly twisted form. The imidazole units lie on opposite sides and the four isopropyl groups all point the same direction. The dihedral angle $\theta_{\text{CR}-\text{C}-\text{CR}}$ is 63° for the *P* isomer, and for the *M* isomer a dihedral angle of -53° is found.

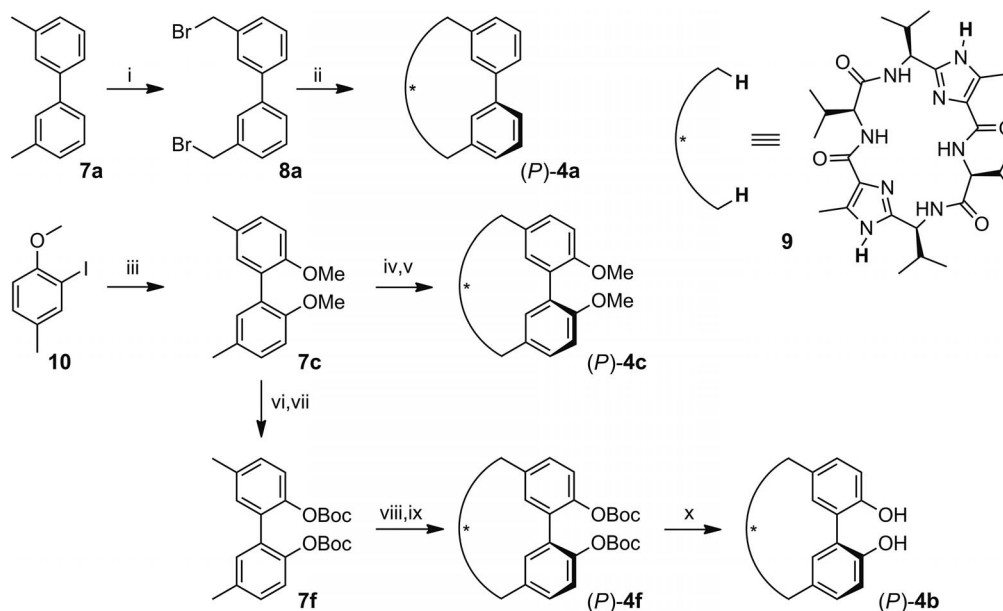
Besides the dihedral angle $\theta_{\text{CR}-\text{C}-\text{CR}}$, the conformers differ in the relative distance between the protons of the biphenyl units (e.g. H2 and H3) and the protons of the peptidic scaffold (see Figure 2). For example, in the *P* conformer, the proton H2 is almost equidistant from the benzylic protons H1a and H1b. In the *M* isomer, the proton H2

points toward the methyl group of the imidazole. Therefore, the distance between H2 and H1b is much smaller than that between H2 and H1a.

Because of this encouraging calculation result, we decided to synthesize selected compounds of the most promising type **4** (bridge **A**) and to check if conformational control in this *tropos* systems is possible.

Synthesis

The syntheses of compounds **4a–c** and **4f** are illustrated in Scheme 2. The synthesis of **4a** starts with dibromination of 3,3'-dimethylbiphenyl (**7a**) using the procedure of Wohl and Ziegler.^[18] The subsequent reaction of the dibromide **8a** with the macrocyclic peptide **9** led to the desired biphenyl



Scheme 2. Preparation of the biphenyl derivatives **4a–c** and **4f**. Reaction conditions: i) NBS, AIBN, CCl_4 , Δ , 40%; ii) **9**, Cs_2CO_3 , CH_3CN , Δ , 26%; iii) In, $\text{Pd}(\text{AcO})_2$, LiCl, DMF, Δ , 68%; iv) NBS, AIBN, CCl_4 , Δ , 89%; v) **9**, Cs_2CO_3 , CH_3CN , Δ , 7%; vi) BBr_3 , DCM, 99%; vii) Boc_2O , DMAP, NEt_3 , DCM, 47%; viii) NBS, AIBN, CCl_4 , Δ , 66%; ix) **9**, Cs_2CO_3 , CH_3CN , Δ , 74%; x) TFA, DCM, 48%.

derivative **4a**. The preparation of the biphenyls **4b,c** and **4f** followed the same principle. In the first step, dimethoxybiphenyl **7c** was synthesized starting from the iodide **10** via an indium-catalyzed biaryl coupling reaction.^[19] A subsequent twofold bromination with NBS and reaction with macrocycle **9** under basic condition gave the dimethoxybiphenyl derivative **4c**. Unfortunately, a direct transformation of the dimethoxybiphenyl **4c** into the dihydroxybiphenyl **4b** using BBr_3 in dichloromethane proved to be unsuccessful. In order to obtain the desired dihydroxybiphenyl **4b**, the methoxy group in **7c** was replaced by an OBoc group in two steps leading to biphenyl **7f**. An NBS bromination and treatment of the resulting dibromide with macrocycle **9** in acetonitrile under basic conditions gave the biphenyl **4f** which was transformed into the desired dihydroxybiphenyl **4b** by trifluoroacetic acid in dichloromethane. In sum, we could synthesize the biphenyls **4a–c** and **4f** in a few steps and, with the exception of **4c**, with moderate to good yields. Thus, considering that the chiral bridge **9** is prepared in one step from a commercially available compound, the biphenyl derivative **4b** was synthesized in only six steps in an overall yield of 7%.

Solid State Structure

We were able to obtain crystals suitable for X-ray structure analysis of biphenyl derivative **4a**. It crystallized as a hydrate in the Sohnke space group $P2_1$ with two independent molecules in the asymmetric unit (see Figure 3). In both cases, the biphenyl unit exhibited the *P* conformation. The dihedral angles $\theta_{\text{CH}_2\text{-C-C-CH}}$ were $+22.4(3)^\circ$ and $+36.1(3)^\circ$, respectively. This difference is probably due to interactions of different strength of the aromatic units in solid state. A comparison of the solid state structures with the calculated structure of (*P*)-**4a** showed that the method B3LYP/6-31G* was indeed suitable for reproducing the binding situation, the conformation and the spatial structure (see also Table 2). Like in the calculated structure, the solid state molecules showed a peptidic scaffold which featured a bowl-like and slightly twisted conformation and in which the imidazole units lay on opposite sides. This structure type was also found in other imidazole-containing cyclic peptides.^[20]

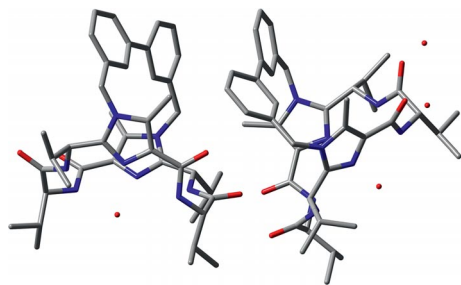


Figure 3. Molecular structure of **4a** in the solid state; both molecules of **4a** in the unit cell are depicted. All hydrogen atoms and some solvent molecules have been omitted for clarity.

NMR Experiments

In the NMR spectra of **4a–c** and **4f**, only single sets of signals were found. There could be two explanations for this observation: either **4a–c** and **4f** undergo a rapid change of conformation (epimerization), or they exist only in a single conformation. In the case of the biphenyl **4a**, which features only hydrogen atoms in the *ortho* and *ortho'* positions, the rotation barrier could be so low that the appearance of two sets of signals in the NMR spectrum would be unexpected. Different behavior is expected for the disubstituted biphenyls **4b–c** and **4f**. Similar *ortho,ortho'*-disubstituted *tropos* biphenyls with a bridge in *meta* position, as well as trisubstituted *tropos* biphenyls without a bridge show two sets of signals in the NMR spectrum,^[7,12] one for each diastereomer. In order to rule out a fast conformational change in solution, VT-NMR experiments for **4a–c** were performed, and 2D-NMR spectra of **4a–c** and **4f** were recorded. They show that no molecular conformational changes occur between -50 and $+50^\circ\text{C}$. Furthermore, the data obtained from the NOESY spectra were used to determine the conformation of the biphenyl units in **4a–c** and **4f**. Important criteria for the discrimination between the *P* and the *M* conformers are the distances H2–H4 and H3–H4 (for numbering of the protons see Figure 2). In the *M* conformer, the proton H2 points toward the methyl group attached at the imidazole (H4), and thus H2 and H3 should be almost equidistant from the methyl group of the imidazole. In the *P* isomer, the phenyl rings are tilted in such a way that the distance between the proton H3 and the protons of the methyl group (H4) is smaller than that between proton H2 and the methyl group (H4). A comparison between the calculated values and the values obtained from the NOESY data makes obvious that the distance H3–H4 is distinctly smaller than H2–H4 (see Table 2). Although the distances obtained by NOESY experiments need to be handled with some care, there is evidence that only the *P* conformer is present in solution. Similar behavior is found

Table 2. Atomic distances [\AA] obtained from NMR spectroscopic experiments, X-ray data and ab initio calculations (B3LYP/6-31G*) for **4a**. The numbering of the protons in **4a** is equivalent to that in **4c** (see Figure 2).

	Atomic distance [\AA], determined by			
	NMR	calculation using B3LYP/6-31G*	X-ray ^[a]	
	4a	(<i>M</i>)- 4a	(<i>P</i>)- 4a	(<i>P</i>)- 4a
H2–H5	2.33 ^[b]	2.48	2.48	2.33
H1a–H2	2.96	3.32	2.76	2.67
H1b–H2	2.83	2.33	2.64	2.57
H1a–H3	3.24	2.97	3.52	3.45
H1b–H3	3.50	3.78	3.58	3.44
H2–H4	4.18	3.30	4.23	3.98
H3–H4	2.68	3.27	2.71	2.80
H1a–H4	4.18	4.07	4.04	3.86
H1b–H4	2.66	2.75	2.67	2.62

[a] Mean values were used. [b] In the case of the NOESY spectra, the distance between the protons H2 and H5 was used as the reference distance for calibration.

for the biphenyls **4b,c** and **4f**, which means that in all cases the *P* conformation is adopted in solution.

CD Spectroscopic Investigations

To confirm the results from the NMR experiments, CD spectroscopic measurements were performed.^[13] For this purpose, the CD spectra of **4a–c** and **4f** in acetonitrile as solvent were recorded. The CD spectra of **4a** and **4c** are depicted in Figure 4 (a), and the CD spectra of **4b** and **4f** are shown in the Supporting Information. Additionally, the CD spectra of (*P*)-**4a**, (*P*)-**4c**, (*M*)-**4a** and (*M*)-**4c** were simulated with the time-dependent density functional theory

(TD-DFT) with B3LYP as the functional and by employing the 6-31G* basis set.

The TD-DFT calculations were performed at the optimized geometries of (*P*)-**4a**, (*P*)-**4c**, (*M*)-**4a** and (*M*)-**4c**, and the simulated CD spectra of the conformers are depicted in parts b and c of Figure 4. In order to determine the conformations of the biphenyl units on the basis of the CD spectra, all transitions which are characteristic for the biphenyl unit were examined. If the dihedral angle between the phenyl units in biphenyl is unequal to 90°, there is a conjugation between the phenyl units and thus the HOMO and LUMO of biphenyl are not degenerate.^[21] A schematic representation of the π MOs of a biphenyl unit exhibiting conjugation between the phenyl units is depicted in Figure 5. It can be assumed that the first absorption band of biphenyl is approximately the electronic transition from ϕ_6 to ϕ_7 .

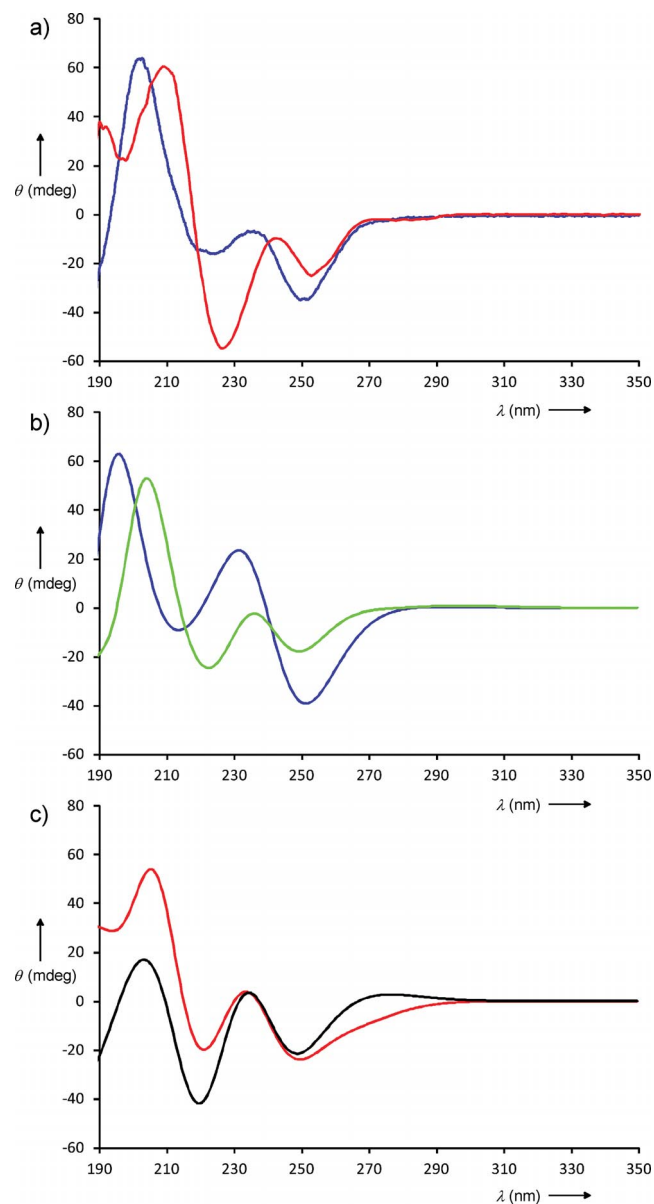


Figure 4. a) Experimentally determined spectra of **4a** (blue: $c = 1.0 \times 10^{-5}$ M in CH_3CN) and **4c** (red: $c = 2.5 \times 10^{-4}$ M in CH_3CN). b) TD-DFT-B3LYP/6-31G* simulated CD spectra of (*P*)-**4a** (blue) and (*M*)-**4a** (green). c) TD-DFT-B3LYP/6-31G* simulated CD spectra of (*P*)-**4c** (red) and (*M*)-**4c** (black).

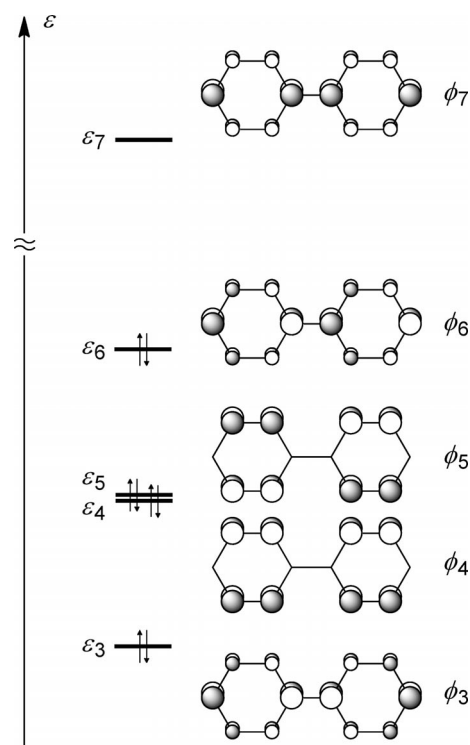


Figure 5. Schematic representation of the π MOs of a biphenyl unit exhibiting conjugation between the phenyl units.

In compounds **4**, the biphenyl units are connected to the peptidic scaffold by methylene groups. Thus, one can expect that the electronic transition from orbital ϕ_6 to ϕ_7 is minimally influenced by the peptidic scaffold. Energy, oscillator strength and rotatory strength are mainly dependent on the substituents of the biphenyl and the size and sign (plus or minus) of the dihedral angle. From the latter, the conformation (*P* or *M*) of the biphenyl can be determined. Therefore, we searched in the simulated CD spectra for those bands which correlate to the electronic transition from ϕ_6 to ϕ_7 of a biphenyl unit and compared them to the experimentally measured ones.

In the case of **4c**, the biphenyl orbital ϕ_6 is energetically raised by conjugation with the nonbonded electron pairs of the methoxy groups and represents the HOMO–1 of (*M*)-**4c** and the HOMO of (*P*)-**4c** (illustrations of these orbitals are depicted in the Supporting Information). According to the DFT calculations, the biphenyl orbital ϕ_7 corresponds to the LUMO of (*M*)-**4c** and to the LUMO of (*P*)-**4c**. The electronic transition from the HOMO of (*P*)-**4c** [HOMO–1 of (*M*)-**4c**] to LUMO is the lowest-energy transition, and is found at 279.3 nm for (*P*)-**4c** and at 272.1 nm for (*M*)-**4c**. The calculated rotatory strength is in both cases relatively small. For (*P*)-**4c**, the calculated value amounts to -12.4×10^{-40} erg-esu-cm/Gauss, and accordingly, a weak negative Cotton effect is found at 280 nm (Figure 4, c). For (*M*)-**4c**, a value of $+14.1 \times 10^{-40}$ erg-esu-cm/Gauss is calculated, which leads to a positive Cotton effect in the simulated spectrum (Figure 4, c). In the experimentally obtained spectrum, a small but negative Cotton effect is observed at 280 nm. Thus, according to the CD spectrum, the biphenyl **4c** adopts the *P* conformation in solution.

In biphenyl **4a**, the biphenyl orbitals ϕ_6 and ϕ_7 correlate to the HOMO–4 and LUMO, respectively, of **4a** (see Supporting Information). The electronic transition from ϕ_6 to ϕ_7 is no longer the lowest-energy one. In the case of (*M*)-**4a**, the calculated value amounts to 256.7 nm and exhibits a rotatory strength of medium size ($+43.9 \times 10^{-40}$ erg-esu-cm/Gauss). In the spectral region around 257 nm, further bands were found, and some of them show negative rotatory strengths. This leads to a negative Cotton effect at 250 nm in the simulated spectrum that is smaller than the one found at about 220 nm (Figure 4, c). For the *P* isomer, the electronic transition from the biphenyl orbital ϕ_6 to the biphenyl orbital ϕ_7 is found at a calculated value of 252.0 nm. The rotatory strength of this transition is strongly negative (-198.9×10^{-40} erg-esu-cm/Gauss) and dominates the area around 250 nm. Accordingly, in the simulated spectrum of (*P*)-**4a**, the negative Cotton effect at 252 nm is distinctly more pronounced than the one at 220 nm. The measured spectrum shows exactly the same pattern: a strong negative Cotton effect at 252 nm caused by the electronic transition from the biphenyl orbital ϕ_6 to the biphenyl orbital ϕ_7 . Once again, the CD spectrum confirms that the biphenyl **4a** adopts the *P* conformation in solution.

Conclusions

In sum, using DFT calculations, we were able to propose a biphenyl system having small substituents in the *ortho* and *ortho'* positions which should be *tropos* and conformationally stable. After successful syntheses, the *tropos* biphenyl derivatives were investigated using VT-NMR, 2D-NMR and CD spectroscopy. We were able to prove that all the biphenyl derivatives adopted the *P* conformation independently of the size of the substituents in the *ortho* and *ortho'* positions. The calculated and measured dihedral angles were distinctly smaller than those of the corresponding con-

formationally stable *atropis* systems. This concept should allow us to develop a series of chiral ligands which are conformationally stable and exhibit small bite angles.

Experimental Section

General Remarks: All chemicals were reagent grade and were used as purchased. Reactions were monitored by TLC analysis with silica gel 60 F254 thin-layer plates. Flash chromatography was carried out on silica gel 60 (230–400 mesh). ^1H and ^{13}C NMR spectra were measured with Bruker Avance DMX 300 and Avance DRX 500 spectrometers. All chemical shifts (δ) are given in ppm relative to TMS. The spectra were referenced to deuterated solvents indicated in brackets in the analytical data. HRMS spectra were recorded with a Bruker BioTOF III Instrument. UV/Vis absorption spectra were obtained with Jasco J-815 and V-550 spectrophotometers. CD absorption spectra were recorded with a Jasco J-815 spectrophotometer.

Biphenyl System 4a: The imidazole macrocycle **9** (27 mg, 0.048 mmol), the dibromide **8a** (16 mg, 0.048 mmol) and cesium carbonate (130 mg, 0.400 mmol) were dissolved in acetonitrile (35 mL) under argon. The reaction mixture was placed in a 90 °C oil bath and was stirred for two hours. After cooling to room temp., the solution was poured into an ethyl acetate/water mixture. The organic phase was separated, dried with magnesium sulfate, and the solvent was removed in vacuo. The residue was purified by column chromatography over silica gel (DCM/AcOEt, 75:25). The product was obtained as a colorless solid (9.0 mg, 26%). Single crystals suitable for X-ray diffraction were obtained by crystallization from acetonitrile at room temperature. ^1H NMR (500 MHz, CDCl_3): δ = 7.45–7.42 (m, 2 H, H_{Ph}), 7.39 (d, $^3J_{\text{H,H}} = 7.7$ Hz, 2 H, H_{Ph}), 7.36 (d, $^3J_{\text{H,H}} = 9.8$ Hz, 2 H, NH), 7.21 (d, $^3J_{\text{H,H}} = 7.9$ Hz, 2 H, H_{Ph}), 6.98 (d, $^3J_{\text{N,H}} = 5.0$ Hz, 2 H, NH), 5.62 (s, 2 H, H_{Ph}), 5.34 (d, $^2J_{\text{H,H}} = 18.0$ Hz, 2 H, $\text{CH}_2\text{-Ph}$), 5.00 (d, $^2J_{\text{H,H}} = 18.0$ Hz, 2 H, $\text{CH}_2\text{-Ph}$), 4.85 [dd, $^3J_{\text{H,H}} = 4.9$, 5.4 Hz, 2 H, $\text{NH-CH-CH}(\text{CH}_3)_2$], 4.38 (dd, $^3J_{\text{H,H}} = 8.5$, 9.8 Hz, 2 H, NH-CH-CO), 2.64–2.58 [m, 2 H, $\text{CH}(\text{CH}_3)_2$], 2.26–2.19 [m, 2 H, $\text{CH}(\text{CH}_3)_2$], 2.21 (s, 6 H, imidazole- CH_3), 1.23 (d, $^3J_{\text{H,H}} = 6.8$ Hz, 6 H, CH-CH_3), 1.20 (d, $^3J_{\text{H,H}} = 6.8$ Hz, 6 H, CH-CH_3), 0.89 (d, $^3J_{\text{H,H}} = 7.1$ Hz, 6 H, CH-CH_3), 0.87 (d, $^3J_{\text{H,H}} = 7.3$ Hz, 6 H, CH-CH_3) ppm. ^{13}C NMR: (125 MHz, CDCl_3): δ = 171.6 (q; C=O), 163.7 (q; C=O), 144.9 (q; $\text{C}_{\text{imidazoleCH}}$), 141.6 (q; C_{Ph}), 135.3 (q; $\text{C}_{\text{imidazoleCH}_3}$), 135.0 (q; C_{Ph}), 129.8 (q; $\text{C}_{\text{imidazoleCO}}$), 129.5 (t; C_{Ph}), 127.4 (t; C_{Ph}), 125.1 (t; C_{Ph}), 120.8 (t; C_{Ph}), 61.1 (t; COCHNH), 51.7 (t; imidazoleCHNH), 46.9 (s; CH_2Ph), 32.4 [t; imidazoleCHCH(CH_3) $_2$], 30.5 [t; $\text{COCHCH}(\text{CH}_3)_2$], 19.7 [p; $\text{COCHCH}(\text{CH}_3)_2$], 19.6 [p; $\text{COCHCH}(\text{CH}_3)_2$], 18.8 [p; imidazoleCHCH(CH_3) $_2$], 17.1 [p; imidazoleCHCH(CH_3) $_2$], 10.3 (p; imidazole CH_3) ppm. IR (ATR): $\tilde{\nu}$ = 2961, 2925, 2873, 1664, 1592, 1500, 1466, 1388, 1339, 1254, 1221, 1197, 1107, 893, 780, 398 cm^{-1} . UV/Vis (CH_3CN): λ_{max} ($\log \epsilon$) = 244 (3.65) nm. CD (CH_3CN): λ ($\Delta \epsilon \text{ mol}^{-1} \text{ dm}^3 \text{ cm}^{-1}$) = 252 (–89.9), 237 (–18.4), 223 (–46.3), 203 (+196.7) nm. HRMS (ESI): calcd. for $\text{C}_{42}\text{H}_{54}\text{N}_8\text{O}_4$ [$\text{M} + \text{H}$] $^+$ 735.4341; found 735.4363; calcd. for [$\text{M} + \text{Na}$] $^+$ 757.4160; found 757.4177.

Biphenyl System 4c: The imidazole macrocycle **9** (60 mg, 0.108 mmol), the dibromide **8c** (112 mg, 0.280 mmol) and cesium carbonate (333 mg, 1.022 mmol) were dissolved in acetonitrile (60 mL) under argon. The reaction mixture was placed in a 90 °C oil bath and was stirred for two hours. After cooling to room temperature, the solution was poured into an ethyl acetate/water mixture. The organic phase was separated, dried with magnesium sulf-

ate and the solvent was removed in vacuo. The residue was purified by column chromatography over silica gel (DCM/AcOEt, 75:25) and subsequently by HPLC. The product was obtained as a colorless solid (6 mg, 7%). ^1H NMR (500 MHz, CDCl_3): δ = 7.34 (d, $^3J_{\text{N,H}} = 10.1$ Hz, 2 H, NH), 7.17 (dd, $^3J_{\text{H,H}} = 8.4$, $^4J_{\text{H,H}} = 2.5$ Hz, 2 H, H_{Ph}), 6.94 (d, $^3J_{\text{H,H}} = 8.4$ Hz, 2 H, H_{Ph}), 6.86 (d, $^3J_{\text{N,H}} = 5.2$ Hz, 2 H, NH), 5.35 (d, $^4J_{\text{H,H}} = 2.2$ Hz, 2 H, H_{Ph}), 5.17 (d, $^2J_{\text{H,H}} = 17.2$ Hz, 2 H, $\text{CH}_2\text{-Ph}$), 5.00 (d, $^2J_{\text{H,H}} = 17.2$ Hz, 2 H, $\text{CH}_2\text{-Ph}$), 4.74 [dd, $^3J_{\text{H,H}} = 5.0$, $^3J_{\text{H,H}} = 4.4$ Hz, 2 H, NH-CH-CH(CH_3)], 4.40 (dd, $^3J_{\text{H,H}} = 9.9$, $^3J_{\text{H,H}} = 8.5$ Hz, 2 H, NH-CH-CO), 3.74 (s, 6 H, OCH_3), 2.65–2.59 [m, 2 H, $\text{CH}(\text{CH}_3)_2$], 2.39 (s, 6 H, imidazole- CH_3), 2.24–2.18 [m, 2 H, $\text{CH}(\text{CH}_3)_2$], 1.20 (d, $^3J_{\text{H,H}} = 6.5$ Hz, 6 H, CH- CH_3), 1.17 (d, $^3J_{\text{H,H}} = 6.9$ Hz, 6 H, CH- CH_3), 0.88 (d, $^3J_{\text{H,H}} = 6.6$ Hz, 6 H, CH- CH_3), 0.84 (d, $^3J_{\text{H,H}} = 6.8$ Hz, 6 H, CH- CH_3) ppm. ^{13}C NMR: (125 MHz, CDCl_3): δ = 171.4 (q; C=O), 163.6 (q; C=O), 157.1 (q; $\text{C}_{\text{Ph}}\text{OCH}_3$), 144.7 (q; $\text{C}_{\text{imidazole}}\text{CH}$), 135.2 (q; $\text{C}_{\text{imidazole}}\text{CH}_3$), 129.5 (q; $\text{C}_{\text{imidazole}}\text{CO}$), 128.5 (q; $\text{C}_{\text{Ph}}\text{Ph}$), 126.6 (t; C_{Ph}), 126.3 (q; $\text{CHC}_{\text{Ph}}\text{CHCH}$), 124.7 (t; $\text{CC}_{\text{Ph}}\text{C}$), 111.9 (t; C_{Ph}), 60.6 (t; COCHNH), 55.9 (p; OCH_3), 51.7 (t; imidazoleCHNH), 46.1 (s; CH_2Ph), 32.1 [t; imidazoleCHCH(CH_3)], 30.6 [t; COCHCH(CH_3)], 19.6 [p; COCHCH(CH_3)], 19.4 [p; COCHCH(CH_3)], 18.71 [p; imidazoleCHCH(CH_3)], 17.1 [p; imidazoleCHCH(CH_3)], 10.0 (p; imidazole CH_3) ppm. IR (ATR): $\tilde{\nu}$ = 3373, 2962, 2930, 2873, 1666, 1591, 1500, 1462, 1420, 1388, 1343, 1246, 1189, 1133, 1087, 1026, 956, 889, 809, 751 cm^{-1} . UV/Vis (CH_3CN): λ_{max} (log ϵ) = 285 (3.39), 249 (3.87), 215 (4.15), 194 (4.29) nm. CD (DCM): λ ($\Delta\epsilon$ $\text{mol}^{-1} \text{dm}^3 \text{cm}^{-1}$) = 274 (−0.6), 253 (−7.6), 242 (−2.9), 225 (−16.0), 209 (+18.3) nm. HRMS (ESI): calcd. for $\text{C}_{44}\text{H}_{58}\text{N}_8\text{O}_6$ [$\text{M} + \text{H}$] $^+$ 795.4551; found 795.4592; calcd. for [$\text{M} + \text{Na}$] $^+$ 817.4372; found 817.4422.

Biphenyl System 4f: The imidazole macrocycle **9** (17 mg, 0.031 mmol), the dibromide **8f** (24 mg, 0.042 mmol) and cesium carbonate (99 mg, 0.304 mmol) were dissolved in acetonitrile (60 mL) under argon. The reaction mixture was placed in a 90 °C oil bath and was stirred for four hours. After cooling to room temperature, the solution was poured into an ethyl acetate/water mixture. The organic phase was separated, dried with magnesium sulfate, and the solvent was removed in vacuo. The residue was purified by column chromatography over silica gel (DCM/AcOEt/MeOH, 75:25:5) and subsequently by HPLC. The product was obtained as a colorless solid (22 mg, 74%). ^1H NMR (500 MHz, CDCl_3): δ = 7.34 (d, $^3J_{\text{N,H}} = 9.9$ Hz, 2 H, NH), 7.25 (d, $^3J_{\text{H,H}} = 8.0$ Hz, 2 H, H_{Ph}), 7.21 (dd, $^3J_{\text{H,H}} = 8.3$, $^4J_{\text{H,H}} = 2.0$ Hz, 2 H, H_{Ph}), 6.89 (d, $^3J_{\text{H,H}} = 5.4$ Hz, 2 H, NH), 5.51 (d, $^4J_{\text{H,H}} = 1.9$ Hz, 2 H, H_{Ph}), 5.24 (d, $^2J_{\text{H,H}} = 17.5$ Hz, 2 H, $\text{CH}_2\text{-Ph}$), 5.01 (d, $^2J_{\text{H,H}} = 17.8$ Hz, 2 H, $\text{CH}_2\text{-Ph}$), 4.78–4.77 [m, 2 H, NH-CH-CH(CH_3)], 4.42–4.38 (m, 2 H, NH-CH-CO), 2.67–2.61 [m, 2 H, $\text{CH}(\text{CH}_3)_2$], 2.38 (s, 6 H, imidazole- CH_3), 2.25–2.18 [m, 2 H, $\text{CH}(\text{CH}_3)_2$], 1.33 [s, 18 H, $\text{PhO}(\text{CO})\text{OC}(\text{CH}_3)_3$], 1.20 (d, $^3J_{\text{H,H}} = 6.8$ Hz, 6 H, CH- CH_3), 1.18 (d, $^3J_{\text{H,H}} = 6.8$ Hz, 6 H, CH- CH_3), 0.88 (d, $^3J_{\text{H,H}} = 6.9$ Hz, 6 H, CH- CH_3), 0.85 (d, $^3J_{\text{H,H}} = 6.9$ Hz, 6 H, CH- CH_3) ppm. ^{13}C NMR: (125 MHz, CDCl_3): δ = 171.62 (q; C=O), 163.43 (q; C=O), 150.36 [q; $\text{O}(\text{C}=\text{O})\text{O}$], 148.03 (q; C_{Ph}), 144.61 (q; $\text{C}_{\text{imidazole}}\text{CH}$), 135.11 (q; $\text{C}_{\text{imidazole}}\text{CH}_3$), 132.39 (q; $\text{C}_{\text{Ph}}\text{Ph}$), 131.26 (q; $\text{C}_{\text{Ph}}\text{CH}_2$), 129.75 (q; $\text{C}_{\text{imidazole}}\text{CO}$), 126.12 (t; C_{Ph}), 125.58 (t; C_{Ph}), 123.31 (t; C_{Ph}), 82.85 [q; $\text{C}(\text{CH}_3)_3$], 60.72 (t; COCHNH), 51.84 (t; imidazoleCHNH), 46.1 (s; CH_2Ph), 32.14 [t; imidazoleCHCH(CH_3)], 30.57 [t; COCHCH(CH_3)], 27.43 [p; $\text{PhO}(\text{CO})\text{OC}(\text{CH}_3)_3$], 19.65 [p; COCHCH(CH_3)], 19.51 [p; COCHCH(CH_3)], 18.84 [p; imidazoleCHCH(CH_3)], 17.05 [p; imidazoleCHCH(CH_3)], 9.79 (p; imidazole CH_3) ppm. IR (ATR): $\tilde{\nu}$ = 3357, 2963, 2929, 2873, 1759, 1666, 1593, 1501, 1462, 1423, 1390, 1370, 1344, 1276, 1250, 1218, 1147, 1051, 945, 891, 811, 776, 737 cm^{-1} . UV/Vis (CH_3CN): λ_{max}

(log ϵ) = 240 (3.31) nm. CD (DCM): λ ($\Delta\epsilon$ $\text{mol}^{-1} \text{dm}^3 \text{cm}^{-1}$) = 251 (−36.0), 237 (−7.3), 220 (−82.3), 203 (+124.8) nm. HRMS (ESI): calcd. for $\text{C}_{52}\text{H}_{70}\text{N}_8\text{O}_{10}$ [$\text{M} + \text{H}$] $^+$ 967.5288; found 967.5288; calcd. for [$\text{M} + \text{Na}$] $^+$ 989.5107; found 989.510; calcd. for [$2\text{M} + \text{Na}$] $^+$ 1957.0328; found 1957.0356.

Biphenyl System 4b: The biphenyl system **4f** (18 mg, 0.019 mmol) was dissolved in dichloromethane (10 mL), and trifluoroacetic acid (0.1 mL, 1.307 mmol) was added. The solution was stirred for two days at room temperature, and afterwards poured into a dichloromethane/water mixture. The organic layer was separated, dried with magnesium sulfate and the solvent was removed in vacuo. The residue was purified by column chromatography over silica gel (DCM/AcOEt/MeOH, 75:25:3) and subsequently by HPLC. The product was obtained as a colorless solid (7 mg, 48%). ^1H NMR (500 MHz, $[\text{D}_4]\text{MeOD}$): δ = 7.19 (dd, $^3J_{\text{H,H}} = 8.2$, $^4J_{\text{H,H}} = 2.4$ Hz, 2 H, H_{Ph}), 6.87 (d, $^3J_{\text{H,H}} = 8.4$ Hz, 2 H, H_{Ph}), 5.44 (d, $^4J_{\text{H,H}} = 2.0$ Hz, 2 H, H_{Ph}), 5.30 (d, $^2J_{\text{H,H}} = 17.8$ Hz, 2 H, $\text{CH}_2\text{-Ph}$), 5.11 (d, $^2J_{\text{H,H}} = 17.3$ Hz, 2 H, $\text{CH}_2\text{-Ph}$), 4.85–4.84 [m, 2 H, NH-CH-CH(CH_3)], 4.19 (d, $^3J_{\text{H,H}} = 11.2$ Hz, 2 H, NH-CH-CO), 2.34–2.24 [m, 4 H, $\text{CH}(\text{CH}_3)_2$], 2.32 (s, 6 H, imidazole- CH_3), 1.20 (d, $^3J_{\text{H,H}} = 6.5$ Hz, 6 H, CH- CH_3), 1.14 (d, $^3J_{\text{H,H}} = 6.6$ Hz, 6 H, CH- CH_3), 0.95 (d, $^3J_{\text{H,H}} = 6.9$ Hz, 6 H, CH- CH_3), 0.9 (d, $^3J_{\text{H,H}} = 6.9$ Hz, 6 H, CH- CH_3) ppm. ^{13}C NMR (125 MHz, $[\text{D}_4]\text{MeOD}$): δ = 174.50 (q; C=O), 166.60 (q; C=O), 155.53 (q; $\text{C}_{\text{Ph}}\text{-OH}$), 146.61 (q; $\text{C}_{\text{imidazole}}\text{CH}$), 137.00 (q; $\text{C}_{\text{imidazole}}\text{CH}_3$), 130.58 (q; $\text{C}_{\text{imidazole}}\text{CO}$), 128.22 (q; $\text{C}_{\text{Ph}}\text{CH}_2$), 128.02 (t; C_{Ph}), 127.86 (q; $\text{C}_{\text{Ph}}\text{Phenyl}$), 126.35 (t; C_{Ph}), 118.01 (t; C_{Ph}), 63.65 (t; COCHNH), 52.81 (t; imidazoleCHNH), 47.33 (s; CH_2Ph), 35.43 [t; $\text{CHCH}(\text{CH}_3)_2$], 31.32 [t; $\text{CHCH}(\text{CH}_3)_2$], 21.20 [p; $\text{CH}(\text{CH}_3)_2$], 20.08 [p; $\text{CH}(\text{CH}_3)_2$], 18.96 [p; $\text{CH}(\text{CH}_3)_2$], 18.75 [p; $\text{CH}(\text{CH}_3)_2$], 10.30 (p; imidazole CH_3) ppm. IR (ATR): $\tilde{\nu}$ = 3353, 2962, 2927, 1656, 1591, 1499, 1463, 1421, 1388, 1372, 1342, 1261, 1239, 1136, 1115, 1027, 995, 944, 892, 812, 780, 722 cm^{-1} . UV/Vis (CH_3CN): λ_{max} (log ϵ) = 337 (1.85), 288 (2.58), 245 (3.31), 217 (3.51) nm. CD (DCM): λ ($\Delta\epsilon$ $\text{mol}^{-1} \text{dm}^3 \text{cm}^{-1}$) = 284 (−4.5), 273 (−3.3), 251 (−32.7), 240 (−19.0), 225 (−57.0), 209 (+88.3) nm. HRMS (ESI): calcd. for $\text{C}_{42}\text{H}_{54}\text{N}_8\text{O}_6$ [$\text{M} + \text{H}$] $^+$ 767.4238; found 767.4238; calcd. for [$\text{M} + \text{Na}$] $^+$ 789.4059; found 789.4061.

Crystal Structure Analysis of 4a: The crystal was mounted on nylon loops in inert oil. Data were collected with a Bruker AXS D8 Kappa diffractometer with an APEX2 detector (monochromated Mo- K_α radiation, $\lambda = 0.71073$ Å) at 100 K. The structures were solved by direct methods (SHELXS-97)^[22] and refined anisotropically by full-matrix least-squares on F^2 (SHELXL-97).^[23] Absorption corrections were performed semiempirically from equivalent reflections on the basis of multiple scans (Bruker AXS APEX2). Hydrogen atoms were refined using a riding model or rigid methyl groups. Hydrogen atom positions of OH and NH groups were taken from a Fourier difference map and refined freely with an isotropic displacement parameter constrained to 1.2 and 1.5 fold of the U_{ij} of the corresponding N and O atom, respectively. OH bond lengths and H–O–H bond angles of the water molecules were restrained to be equal (SADI). The absolute structure parameter \times (Flack parameter^[24]) was ambiguous due to the lack of heavy atoms. Consequently, the absolute structure was assigned by reference to a known configuration of a chiral centre that did not change during the syntheses. A selection of crystallographic parameters for compound **4a** are found in Table 3.

CCDC-905893 contains the supplementary crystallographic data for this paper. These data can be obtained free of charge from The Cambridge Crystallographic Data Centre via www.ccdc.cam.ac.uk/data_request/cif.

Table 3. Crystal structure data for compound **4a**.

Formula	C ₄₂ H ₅₄ N ₈ O ₄ ·2(H ₂ O)
M _r	770.96
Crystal size [mm ³]	0.38 × 0.32 × 0.22
T [K]	100(1)
Crystal system	monoclinic
Space group	P2 ₁
a [Å]	10.3904(3)
b [Å]	22.7835(7)
c [Å]	17.9678(5)
β [°]	98.8910(10)
V [Å ³]	4202.4(2)
Z	4
D _{calc} [g cm ⁻³]	1.219
μ(Mo-K _α) [mm ⁻¹]	0.083
Transmissions	0.75/0.57
F(000) [e]	1656
hkl ranges	-13 ≤ h ≤ 12, -22 ≤ k ≤ 29, -22 ≤ l ≤ 23
2θ _{max} [°]	27.18
Reflections collected	80462
Independent reflections	15010
R _{int}	0.0363
Refined parameters	1073
R(F) [F ≥ 4σ(F)] ^[a]	0.0411
wR(F ²) (all data) ^[a]	0.0986
x (Flack)	0.4(6)
GoF (F ²) ^[b]	1.028
Δρ _{fin} (max./min.) [e Å ⁻³]	0.924/-0.258

[a] $R(F) = \frac{\sum \|F_o\| - |F_c|}{\sum \|F_o\|}$; $wR(F^2) = \frac{[\sum \{w(F_o^2 - F_c^2)^2\} / \sum \{w(F_o^2)^2\}]^{0.5}}{[\sum \{w(F_o^2)^2\} + (aP)^2 + bP]^{0.5}}$ with $P = [F_o^2 + 2F_c^2] / 3$, a and b are constants chosen by the program. [b] $\text{GoF} = \frac{[\sum \{w(F_o^2 - F_c^2)^2\} / (n - p)]^{0.5}}{n}$ with n data and p parameters.

Supporting Information (see footnote on the first page of this article): Copies of the ¹H NMR and ¹³C NMR spectra for key intermediates and final products. Synthesis of the compounds **7b–c**, **7f**, **8c** and **8f** and sections from the NOESY spectra of **4a–c** and **4f**. CD spectra of **4b** and **4f**, illustration of key orbitals of **4a** and **4c**.

Acknowledgments

This work was generously supported by the Deutsche Forschungsgemeinschaft (DFG). The authors thank Prof. Günter Helmchen (University of Heidelberg) for helpful discussion.

- [1] a) T. W. Wallace, *Org. Biomol. Chem.* **2006**, *4*, 3197–3210; b) G. Bringmann, A. J. Price Mortimer, P. A. Keller, M. J. Gresser, J. Garner, M. Breuning, *Angew. Chem.* **2005**, *117*, 5518–5563; *Angew. Chem. Int. Ed.* **2005**, *44*, 5384–5427; c) J. Hassan, M. Sévignon, C. Gozzi, E. Schulz, M. Lemaire, *Chem. Rev.* **2002**, *102*, 1359–1469.
- [2] a) S. Schenker, A. Zamfir, M. Freund, S. B. Tsogoeva, *Eur. J. Org. Chem.* **2011**, 2209–2222; b) M. Gaunt, *Nature* **2011**, *470*, 183–185; c) M. Terada, *Synthesis* **2010**, *12*, 1929–1982; d) D. S. Surry, S. L. Buchwald, *Angew. Chem.* **2008**, *120*, 6438–6461; *Angew. Chem. Int. Ed.* **2008**, *47*, 6338–6361; e) T. Akiyama, *Chem. Rev.* **2007**, *107*, 5744–5758; f) R. Noyori, *Angew. Chem.* **2002**, *114*, 2108–2123; *Angew. Chem. Int. Ed.* **2002**, *41*, 2008–2022; g) L. Pu, *Chem. Rev.* **1998**, *98*, 2405–2494; h) R. Noyori, *Asymmetric Catalysis in Organic Synthesis*, Wiley, New York, **1994**.
- [3] a) L. Pu, *Acc. Chem. Res.* **2012**, *45*, 150–163; b) J. Bunzen, T. Bruhn, G. Bringmann, A. Lützen, *J. Am. Chem. Soc.* **2009**, *131*, 3621–3630; c) F. Toda, *Inclusion Compounds*, Vol. 4, Chap. 4 (Eds.: J. L. Atwood, J. E. D. Davies, D. D. MacNicol), Oxford University Press, Oxford, UK, **1991**; d) J. Rebek Jr, T. Costello, L. Marshall, R. Wattle, R. C. Gadwood, K. Onan, *J. Am. Chem. Soc.* **1985**, *107*, 7481–7487; e) E. P. Kyba, G. W. Gokel, F. de Jong, K. Koga, L. R. Sousa, M. G. Siegel, L. Kaplan, G. D. Y. Sogah, D. J. Cram, *J. Org. Chem.* **1977**, *42*, 4173–4184.
- [4] a) L. Meca, D. Řeha, Z. Havlas, *J. Org. Chem.* **2003**, *68*, 5677–5680; b) K. Mikami, K. Aikawa, Y. Yusa, J. J. Jodry, M. Yamana, *Synlett* **2002**, *10*, 1561–1578; c) G. Bott, L. D. Field, S. Sternhell, *J. Am. Chem. Soc.* **1980**, *102*, 5618–5626; d) R. Adams, H. C. Yuan, *Chem. Rev.* **1933**, *33*, 261–338.
- [5] a) M. Oki, *Top. Stereochem.* **1983**, *14*, 1–81; b) M. Oki, G. Yamamoto, *Bull. Chem. Soc. Jpn.* **1971**, *44*, 266–270.
- [6] a) J. M. Brunel, *Chem. Rev.* **2007**, *107*, PR1–PR45; b) J. M. Brunel, *Chem. Rev.* **2005**, *105*, 857–897.
- [7] F. Leroux, *ChemBioChem* **2004**, *5*, 644–649.
- [8] a) A. Leitner, S. Shekhar, M. J. Pouy, J. F. Hartwig, *J. Am. Chem. Soc.* **2005**, *127*, 15506–15514; b) Y. Mata, M. Diéguez, O. Pàmies, C. Claver, *Org. Lett.* **2005**, *7*, 5597–5599; c) M. T. Reetz, X. Li, *Angew. Chem.* **2005**, *117*, 3019–3021; *Angew. Chem. Int. Ed.* **2005**, *44*, 2959–2962.
- [9] a) C. Wang, G. Yang, J. Zhuang, W. Zhang, *Tetrahedron Lett.* **2010**, *51*, 2044–2047; b) Y. J. Zhang, H. Wei, W. Zhang, *Tetrahedron* **2009**, *65*, 1281–1286; c) H. Wei, Y. J. Zhang, Y. Dai, J. Zhang, W. Zhang, *Tetrahedron Lett.* **1996**, *68*, 2193–2222.
- [10] A conformation is defined as the “spatial arrangement of the atoms affording distinction between stereoisomers which can be interconverted by rotations about formally single bonds”. If we comply with this definition, the stereoisomers discussed in this paper are conformers, and accordingly we denote them as *M* and *P* conformers.
- [11] a) J. Etxebarria, H. Degenbeck, A.-S. Felten, S. Serres, N. Nieto, A. Vidal-Ferran, *J. Org. Chem.* **2009**, *74*, 8794–8797; b) S. Wünnemann, R. Fröhlich, D. Hoppe, *Org. Lett.* **2006**, *8*, 2455–2458; c) R. Eelkema, B. L. Feringa, *J. Am. Chem. Soc.* **2005**, *127*, 13480–13481; d) H. Takagi, T. Mizutani, T. Horiguchi, S. Kitagawa, H. Ogoshi, *Org. Biomol. Chem.* **2005**, *3*, 2091–2094.
- [12] a) J. Wang, S. Dong, Y. Wang, Q. Lu, H. Zhong, G. Du, L. Zhang, Y. Cheng, *Bioorg. Med. Chem.* **2008**, *16*, 8510–8515; b) A. Jossang, A. Cavé, J. Saez, M. H. Bartoli, A. Cavé, P. Jossang, *J. Org. Chem.* **1996**, *61*, 3023–3030; c) K. Fujii, T. Yamada, E. Fujita, K. Kuriyama, T. Iwata, M. Shiro, H. Nakai, *Chem. Pharm. Bull.* **1984**, *32*, 55–62.
- [13] M. J. Frisch, G. W. Trucks, H. B. Schlegel, G. E. Scuseria, M. A. Robb, J. R. Cheeseman, J. A. Montgomery Jr., T. Vreven, K. N. Kudin, J. C. Burant, J. M. Millam, S. S. Iyengar, J. Tomasi, V. Barone, B. Mennucci, M. Cossi, G. Scalmani, N. Rega, G. A. Petersson, H. Nakatsuji, M. Hada, M. Ehara, K. Toyota, R. Fukuda, J. Hasegawa, M. Ishida, T. Nakajima, Y. Honda, O. Kitao, H. Nakai, M. Klene, X. Li, J. E. Knox, H. P. Hratchian, J. B. Cross, V. Bakken, C. Adamo, J. Jaramillo, R. Gomperts, R. E. Stratmann, O. Yazyev, A. J. Austin, R. Cammi, C. Pomelli, J. W. Ochterski, P. Y. Ayala, K. Morokuma, G. A. Voth, P. Salvador, J. J. Dannenberg, V. G. Zakrzewski, S. Dapprich, A. D. Daniels, M. C. Strain, O. Farkas, D. K. Malick, A. D. Rabuck, K. Raghavachari, J. B. Foresman, J. V. Ortiz, Q. Cui, A. G. Baboul, S. Clifford, J. Cioslowski, B. B. Stefanov, G. Liu, A. Liashenko, P. Piskorz, I. Komaromi, R. L. Martin, D. J. Fox, T. Keith, M. A. Al-Laham, C. Y. Peng, A. Nanayakkara, M. Challacombe, P. M. W. Gill, B. Johnson, W. Chen, M. W. Wong, C. Gonzalez, J. A. Pople, *Gaussian 03*, rev. C.02, Gaussian, Inc., Wallingford CT, **2004**.
- [14] G. Haberhauer, *Angew. Chem.* **2007**, *119*, 4476–4479; *Angew. Chem. Int. Ed.* **2007**, *46*, 4397–4399.
- [15] a) G. Haberhauer, E. Drosdow, T. Oeser, F. Rominger, *Tetrahedron* **2008**, *64*, 1853–1859; b) G. Haberhauer, A. Pintér, T. Oeser, F. Rominger, *Eur. J. Org. Chem.* **2007**, 1779–1792; c) G. Haberhauer, F. Rominger, *Eur. J. Org. Chem.* **2003**, 3209–3218.
- [16] a) C. Tepper, G. Haberhauer, *Chem. Eur. J.* **2011**, *17*, 8060–8065; b) G. Haberhauer, *Angew. Chem.* **2011**, *123*, 6539–6543; G. Haberhauer, *Angew. Chem.* **2011**, *123*, 6539; *Angew. Chem. Int. Ed.* **2011**, *50*, 6415–6418; c) G. Haberhauer, C. Kallweit,

- Angew. Chem.* **2010**, *122*, 2468–2471; C. Kallweit, *Angew. Chem.* **2010**, *122*, 2468; *Angew. Chem. Int. Ed.* **2010**, *49*, 2418–2421; d) G. Haberhauer, *Angew. Chem.* **2010**, *122*, 9474–9477; G. Haberhauer, *Angew. Chem.* **2010**, *122*, 9474; *Angew. Chem. Int. Ed.* **2010**, *49*, 9286–9289; e) S. Ernst, G. Haberhauer, *Chem. Eur. J.* **2009**, *15*, 13406–13416; f) M. Schnopp, S. Ernst, G. Haberhauer, *Eur. J. Org. Chem.* **2009**, 213–222; g) G. Haberhauer, *Angew. Chem.* **2008**, *120*, 3691–3694; *Angew. Chem. Int. Ed.* **2008**, *47*, 3635–3638; h) G. Haberhauer, T. Oeser, F. Rominger, *Chem. Commun.* **2005**, 2799–2801.
- [17] a) S.-B. Miao, D.-S. Deng, X.-M. Liu, B.-M. Ji, *Acta Crystallogr., Sect. E* **2009**, *65*, o2314; b) G. V. Gridunova, V. E. Shklover, Y. T. Struchkov, B. A. Chayanov, *Kristallografiya* **1983**, *28*, 87–91.
- [18] C. Djerassi, *Chem. Rev.* **1948**, *43*, 271–317.
- [19] P. H. Lee, D. Seomoon, K. Lee, *Org. Lett.* **2005**, *7*, 343–345.
- [20] a) Á. Pintér, G. Haberhauer, *Synlett* **2009**, 3082–3098; b) G. Haberhauer, F. Rominger, *Tetrahedron Lett.* **2002**, *43*, 6335–6338.
- [21] R. Gleiter, G. Haberhauer, *Aromaticity and Other Conjugation Effects*, Wiley-VCH, Weinheim, Germany, **2012**.
- [22] G. M. Sheldrick, *Acta Crystallogr., Sect. A* **1990**, *46*, 467–473.
- [23] G. M. Sheldrick, *SHELXL-97, Program for the Refinement of Crystal Structures*, University of Göttingen, Germany, **1997** (see also: G. M. Sheldrick, *Acta Crystallogr. Sect. A* **2008**, *64*, 112–122); for shelXle, *A Qt GUI for SHELXL*, see: C. B. Hübschle, G. M. Sheldrick, B. Dittrich, *J. Appl. Crystallogr.* **2011**, *44*, 1281–1284.
- [24] H. D. Flack, *Acta Crystallogr., Sect. A* **1983**, *39*, 876–881.

Received: January 17, 2013

Published Online: March 14, 2013